Klemm, Matthias; Sauer, Lydia; Klee, Sascha; Link, Dietmar; Peters, Sven; Hammer, Martin; Schweitzer, Dietrich; Haueisen, Jens:

Bleaching effects and fluorescence lifetime imaging ophthalmoscopy

Original published in:

Biomedical optics express. - Washington, DC : OSA. - 10 (2019), 3, p. 1446-1461.

Original published: March 01, 2019

ISSN: 2156-7085

DOI: 10.1364/BOE.10.001446

[*Visited:* July 08, 2019]

Research Article | Vol. 10, No. 3 | 1 Mar 2019 | BIOMEDICAL OPTICS EXPRESS 1446
Biomedical Optics EXPRESS

Bleaching effects and fluorescence lifetime imaging ophthalmoscopy

MATTHIAS KLEMM,[1,*] LYDIA SAUER,[2,3] SASCHA KLEE,[1] DIETMAR LINK,[1] SVEN PETERS,[2] MARTIN HAMMER,[2,4] DIETRICH SCHWEITZER,[2] AND JENS HAUEISEN[1]

[1]*Institute of Biomedical Engineering and Informatics, Technische Universität Ilmenau, POB 100565, 98694 Ilmenau, Germany*
[2]*University Hospital Jena, Department of Ophthalmology, Am Klinikum 1, 07743 Jena, Germany*
[3]*John A. Moran Eye Center, University of Utah, Salt Lake City, UT, USA*
[4]*University of Jena, Center for Biomedical Optics and Photonics, 07740 Jena, Germany*
** matthias.klemm@tu-ilmenau.de*

Abstract: This study investigates the influence of photopigment bleaching on autofluorescence lifetimes in the fundus in 21 young healthy volunteers. Three measurements of 30° retinal fields in two spectral channels (SSC: 498–560 nm, LSC: 560–720 nm) were obtained for each volunteer using fluorescence lifetime imaging ophthalmoscopy (FLIO). After dark-adaptation by wearing a custom-made lightproof mask for 30 minutes, the first FLIO-measurement was recorded (dark-adapted state). Subsequently, the eye was bleached for 1 minute (luminance: 3200 cd/m^2), followed by a second FLIO-measurement (bleached state). Following an additional 10 minute dark adaptation using the mask, a final FLIO-measurement was recorded (recovered state). Average values of the fluorescence lifetimes were calculated from within different areas of a standardized early treatment diabetic retinopathy study (ETDRS) grid (central area, inner and outer rings). The acquisition time in the bleached state was significantly shortened by approximately 20%. The SSC did not show any significant changes in fluorescence lifetimes with photopigment bleaching, only the LSC showed small but significant bleaching-related changes in the fluorescence lifetimes τ_1 and τ_2 from all regions, as well as the mean fluorescence lifetime in the central area. The fluorescence lifetime differences caused by bleaching were by far less significant than pathological changes caused by eye diseases. The magnitudes of fluorescence lifetime changes are <10% and do not interfere with healthy or disease related FLIO patterns. Thus, we conclude that bleaching is not a relevant confounder in current clinical applications of FLIO.

1. Introduction

Fundus autofluorescence (FAF) intensity imaging has become a well-known diagnostic tool in ophthalmology over the past years [1]. Autofluorescence is generated by endogenous fluorophores in the ocular fundus. A large proportion of the autofluorescence originates from lipofuscin accumulated in the retinal pigment epithelium (RPE) [2], which is a complex mixture of bisretinoid fluorophores [3–5]. Spectrally resolved autofluorescence measurements in human donor eyes revealed the diversity of fluorophores in age-related macular degeneration (AMD) patients and controls [6,7]. The decay of the autofluorescence over time can be measured in vivo using the novel method of fluorescence lifetime imaging ophthalmoscopy (FLIO) [8,9]. As the fluorescence lifetime is characteristic for each fluorophore as well as its molecular environment, FLIO provides additional information compared to FAF intensity imaging. FLIO is able to produce repeatable [10] and quantitative [11] images. It was developed by Schweitzer et al. [12] based on fluorescence lifetime imaging (FLIM) techniques [13] used in microscopy [14]. FLIO contributes significantly to

#344779 https://doi.org/10.1364/BOE.10.001446
Journal © 2019 Received 31 Aug 2018; revised 2 Dec 2018; accepted 2 Dec 2018; published 28 Feb 2019

Biomedical Optics EXPRESS

the early detection of diseases in human eyes, as has been shown for diseases such as AMD [15], diabetic retinopathy [16], and MacTel [17]. It is likely that this novel technique may show changes in the eyes of patients even before permanent morphological damage occurs. FLIO also emerges as a promising tool in basic research, as it may contribute to the understanding of pathologic mechanisms involved in metabolic diseases [18]. Excitation spectra, emission spectra and fluorescence lifetime of endogenous fluorophores at the human ocular fundus are compiled elsewhere [8,18,19].

The visual pigments of photoreceptors are not significantly fluorescent [20]. However, they could influence fluorescence signals measured in a multifluorophore system by a spectrally selective absorption of the fluorescence light. Investigating quantitative FAF, photoreceptors are typically bleached for 20 to 30 seconds prior to the actual measurement [21]. Bleaching reduces the effective photopigment concentration of the photoreceptors, as human photopigments are photolabile. The amount of pigment bleached is proportional to its quantum catch [22]. After successive bleaching exposures, the regeneration of the photopigments can be described by a single exponential function with a time constant of 1 to 2 minutes [23]. Consequently, the fluorescence intensity signal from layers below the photopigments should be stronger if measured directly after bleaching. This may consequently reduce the required acquisition time. The same is likely to hold true for FLIO.

More than 10 known endogenous fluorophores exist in the human retina [18,24,25] but the FLIO technique is currently limited to the simultaneous detection of at most three spatially resolved fluorescence lifetimes. The approximated fluorescence lifetime in FLIO typically does not correspond to a single endogenous fluorophore, as it comprises fluorescence information from multiple retinal fluorophores. Hence, the spectrally selective absorption of light (both, excitation as well as fluorescence light) by photopigments may influence the overall fluorescence lifetime and alter amplitudes of individual fluorophores. Nevertheless, the fluorescence lifetime of endogenous fluorophores is not affected by bleaching.

The aim of this work is to investigate the influence of photopigment bleaching on FLIO measurements in a group of healthy volunteers.

2. Materials and methods

2.1 Participants

Twenty-one volunteers with an average age of 23.6 ± 3.8 years (43% female), a clear crystalline lens, and no history of ocular pathology participated in this study. One eye per volunteer was included, refraction errors less than −6 to +6 diopters were accepted. Normal intraocular pressure was confirmed by noncontact tonometry. All research procedures were performed according to the Declaration of Helsinki. Approval for the study was obtained from the ethics committee of the University Hospital Jena. Written informed consent was obtained from each volunteer prior to participation in the study.

2.2 Study design

Pupils were dilated with 0.5% Tropicamid (Mydriaticum Stulln, Pharma Stulln GmbH, Stulln, Germany), and dark adaptation was achieved with the use of a custom-made lightproof mask, as described below. The FLIO device was adjusted to the volunteer's eye before the dark adaptation phase was started. After 30 min of dark adaptation, the baseline FLIO measurement was recorded, following an exposure to bright light for 1 minute using the below-described bleaching device. Subsequently, a second FLIO recording was immediately performed. The volunteer was then again asked to wear the custom-made lightproof mask for an additional 10 minutes until a final FLIO recording was conducted.

Biomedical Optics EXPRESS

2.3 Instrumentation

A schematic of the FLIO device is shown in Fig. 1, details are described elsewhere [11,25,26].

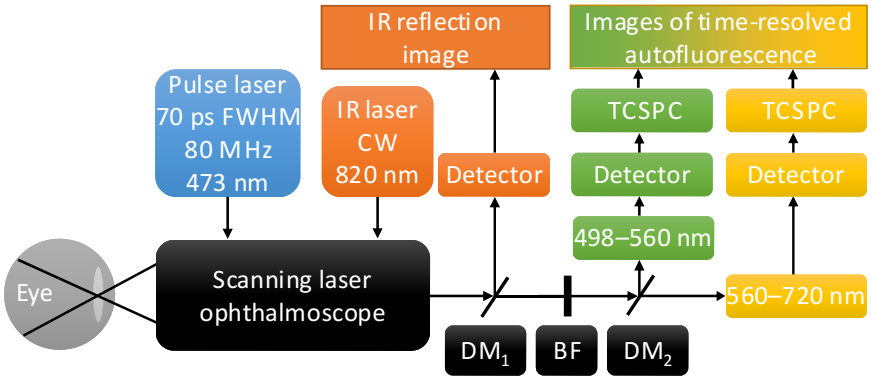

Fig. 1. Schematic of the FLIO instrument. A 473 nm pulsed laser is fed into a scanning laser ophthalmoscope by a monomode fiber to excite retinal autofluorescence. Fluorescence emission is transmitted by a multimode fiber to a dichroic mirror (DM), which divides the fluorescence signal into a short (498–560 nm) and a long spectral channel (560–720 nm). Hybrid photomultiplier tube detectors convert the fluorescence photons into electrical pulses, which are then processed using time-correlated single photon-counting (TCSPC). A continuous wave (CW) infrared (IR) laser illuminates the fundus for online image registration. Blocking filters (BF) protect the detectors from excitation and infrared light.

It is based on a confocal scanning laser ophthalmoscope (cSLO, HRA-2, Heidelberg Engineering GmbH, Heidelberg, Germany). Fundus images (30°, 256 × 256 pixels) are recorded in a high-speed mode at 8.8 frames/s. A pulsed diode laser with a wavelength of 473 nm (BDL-473-SMC, Becker & Hickl GmbH), a pulse width of approximately 89 ps (full-width-at-half-maximum, FWHM), and a repetition rate of 80 MHz is fiber-coupled (single-mode) into the cSLO to excite the autofluorescence. The laser power in the corneal plane is approximately 150 µW, and, according to Sauer et al. [25], it is almost a factor of 10^4 below the exposure limits set by the ANSI standards for durations of up to 8 h [27]. The fluorescence photons are collected by a multimode fiber and split into a short spectral channel (SSC; 498–560 nm) and a long spectral channel (LSC; 560–720 nm) by a dichroic mirror (edge-wavelength 560 nm) after the excitation wavelength was blocked by an edge filter. The detectors (HPM-100-40, Becker & Hickl GmbH) of both channels were connected to a time-correlated single photon-counting (TCSPC) device (SPC-150, Becker & Hickl GmbH). By combining the cSLO and the TCSPC technique [13,28,29] with multiple detectors, FLIO generates time-, space-, and spectrum-resolved fluorescence decay data sets. It takes approximately 2 min for each FLIO measurement to reach the target of 1000 photons per pixel [11] in the macular region in the SSC. The FWHM of the instrument response function (IRF) is 172 ps for the SSC, and 153 ps for the LSC.

To ensure a stringent and smooth measurement and bleaching procedure, it is important to minimize the time interval between the bleaching and the FLIO measurement. Bleaching stimuli were delivered in a customized mini-ganzfeld sphere, which is able to provide the required luminance and can easily be mounted within very close proximity to the chin rest of the FLIO. Figure 2(C) demonstrates the bleaching setup for a right eye using a Styrofoam head model.

Biomedical Optics EXPRESS

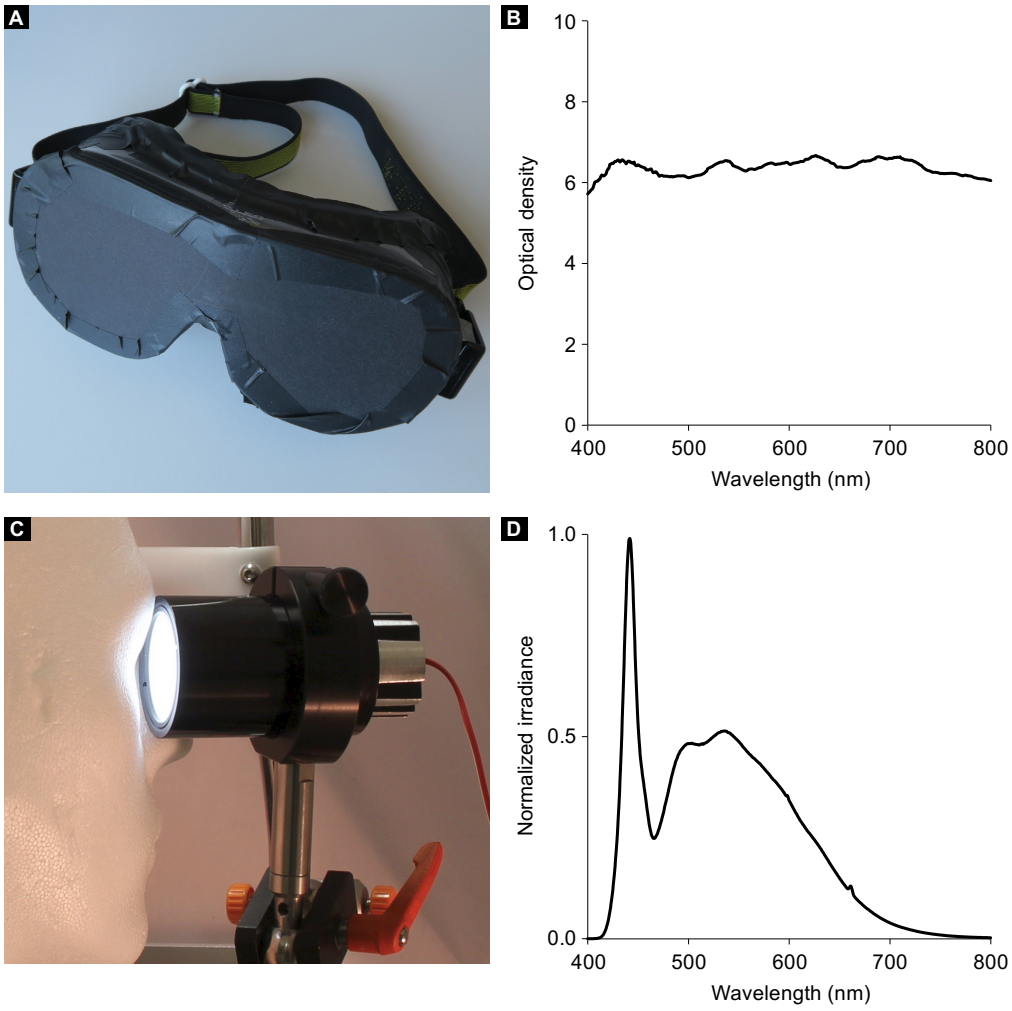

Fig. 2. Custom-made lightproof mask, its optical density, miniaturized bleaching device, and the bleaching spectrum. The custom-made lightproof mask used for dark adaptation is shown in (A). Its optical density is shown in (B). The miniaturized tube-shaped bleaching device (C) consists a high-power white light emitting diode, connected to a standard power supply, a Lambertian-scattering plastic hemisphere (concave against the eye, diameter 40 mm) and a passive aluminum heat sink. The bleaching device was connected to the side of the FLIO device. The bleaching procedure is demonstrated for a right eye using a Styrofoam head model. The effective bleaching spectrum (D) was measured with a scanning spectrometer and a fiber-connected detector. For a bleaching distance of 20 mm (tube edge - cornea), a normalized power of 0.46 mW/cm^2 (corresponds to 1379 lx) was measured. The luminance was 3200 ± 200 cd/m^2.

The custom-made lightproof mask (Fig. 2(A)) was built based on laser protection glasses, which were fortified using multiple layers of blackened paper and black tape. Owing to these measures, an optical density of six was achieved for visible light for the mask (Fig. 2(B)).

The miniaturized tube-shaped bleaching device consists of a high-power, white light, emitting diode (WLED; GW5BTF65K00, Sharp Corporation, Osaka, Japan), a Lambertian-scattering plastic hemisphere, and a passive aluminum heat sink. The WLED acts as backlight behind the hemisphere, which has a diameter of 40 mm, with the concave part facing the eye. The WLED is connected to a standard power supply. Luminance was adjusted to 3200 cd/m^2 by setting the power supply to 8.6 V and 80 mA, it was also measured by a luminance meter (LS-110, Minolta Camera Co. Ltd. Osaka, Japan). The bleaching device was mounted at the

Biomedical Optics EXPRESS

outside of the chin and forehead rest of the FLIO device. Thus, the volunteers simply needed to turn their head for the bleaching procedure. Figure 2(D) shows the normalized, effective bleaching spectrum, in the range of 400 nm to 850 nm. The spectral irradiance E_λ was measured with a scanning spectroradiometer in combination with an integration sphere (Spectro 320 + ISP 75, Instrument Systems GmbH, Munich, Germany). The dilated pupil was assumed to have a maximum diameter of 7 mm. The circular aperture of the integration sphere was 7 mm in diameter and was positioned directly in front of the bleaching device. A normalized power of 0.46 mW/cm^2 was measured at the front of the bleaching device at a bleaching distance of approximately 20 mm between the tube edge and the cornea, which corresponds to 1379 lx. Eye safety for the bleaching device was estimated in accordance to the specified fundamental requirements for optical radiation safety for ophthalmic instruments in humans (Ophthalmic instruments - Fundamental requirements and test methods - Part 2: Light hazard protection (ISO 15004-2:2007)) for continuous-wave operation. The unweighted infrared irradiance at cornea and crystalline lens $E_{IR\text{-}CL}$ is defined as

$$E_{IR-CL} = \sum_{770}^{2500} E_\lambda \cdot \Delta\lambda \tag{1}$$

and results in $E_{IR\text{-}CL}$ = 8.1 x 10^{-5} mW/cm^2, which is a factor of 2.5 x 10^5 below the exposure limit defined by the standard. The weighted visible and infrared irradiance at the retina $E_{VIR\text{-}R}$ is defined as

$$E_{VIR-R} = \sum_{380}^{1400} E_\lambda \cdot R(\lambda) \cdot \Delta\lambda \tag{2}$$

where $R(\lambda)$ is the spectral weighting function for thermal hazard defined by the standard. For the bleaching device used in this work, $E_{VIR\text{-}R}$ = 0.7 x 10^{-5} mW/cm^2, which is a factor of 1.02 x 10^4 below the exposure limit defined by the standard.

As the FLIO device is about a factor of 10^4 below the exposure limit, the consecutive use of FLIO device and bleaching device in the same session is safe according to the standard.

Estimation of the photopigment bleaching level was realized based on an equation proposed by Hollins and Alpern [30], and modified by Paupoo et al. [31], in accordance to,

$$B = \frac{E_v}{E_v + E_{vp}} \cdot \left(1 - e^{-\left(1+\frac{E_v}{E_{vp}}\right)\cdot\frac{t}{\tau_p}} \right) \tag{3}$$

where B is the fraction of photopigment bleached at the end of the bleaching procedure of duration t, with a retinal illumination E_v. E_{vp} is the steady retinal illuminance that bleaches half the pigment, and τ_p is the time constant of photopigment regeneration. Based on the fact that τ_p increases with age, a time constant of 90 s was employed as proposed by Coile and Baker [32] for volunteer ages of approximately 30 years. Several groups have investigated and quantified the value of E_{vp}. These studies have produced variable results that ranged between 20.000 and 30.000 Td [22,30]. Based on these values, the fraction of the bleached photopigment in this work ranged between 83% and 89%. Paupoo et al. [31] also measured the regeneration kinetics of photopigment and found an exponential recovery behavior in accordance to,

$$\frac{r(t)}{r_{\max}} = 1 - B \cdot \mathrm{e}^{-\frac{t}{\tau_p}} \tag{4}$$

where r is the fraction of pigment recovered. Thus, in this work 89% of bleached photopigment is fully recovered after 6 minutes.

Biomedical Optics EXPRESS

2.4 Data analysis

To estimate the fluorescence lifetimes and amplitudes, a multi-exponential approach was used to describe the measured data based on the sum of exponential decay curves according to

$$I(\mathrm{t}) = IRF * \sum_i \alpha_i \cdot e^{-\frac{t}{\tau_i}} + b \tag{5}$$

where I is the time-dependent fluorescence intensity, α is the amplitude, τ is the fluorescence lifetime, i is the index of the exponential, and b is the background, e.g., from thermal noise of the detector or background light. The asterisk denotes a convolution integral. The background is fixed to 0.004 photons per pixel, which was experimentally determined for typical acquisition times in the dark room where all FLIO measurements were conducted. Three exponential functions and a binning with a factor of 2 were applied. To approximate the fluorescence lifetime parameters, the global optimum per pixel, characterized by the smallest possible figure of merit, was determined using a nonlinear optimization algorithm [33]. The χ^2 error according to Neyman's approach [34] was used in its reduced form, χ_r^2, as the figure of merit, and in accordance to,

$$\chi_r^2 = \frac{1}{m-p} \cdot \sum_{j=1}^{m} \frac{\left(I_M(t_j) - I_C(t_j)\right)^2}{I_M(t_j)} \tag{6}$$

where m is the number of time channels of the photon histogram, $I_M(t_j)$ is the number of measured photons, $I_c(t_j)$ is the number of calculated photons estimated using Eq. (5), and p is the number of free parameters in the model.

The amplitude-weighted, mean fluorescence lifetime τ_m was then calculated from the fluorescence amplitudes and lifetimes as

$$\tau_m = \frac{\sum_i \alpha_i \cdot \tau_i}{\sum_i \alpha_i} \tag{7}$$

A standardized early treatment diabetic retinopathy study (ETDRS) grid centered at the macula [35] was placed by an expert in each FLIO measurement. Its central area, as well as inner and outer rings were used for further analyses. This is highlighted in Fig. 3.

Biomedical Optics EXPRESS

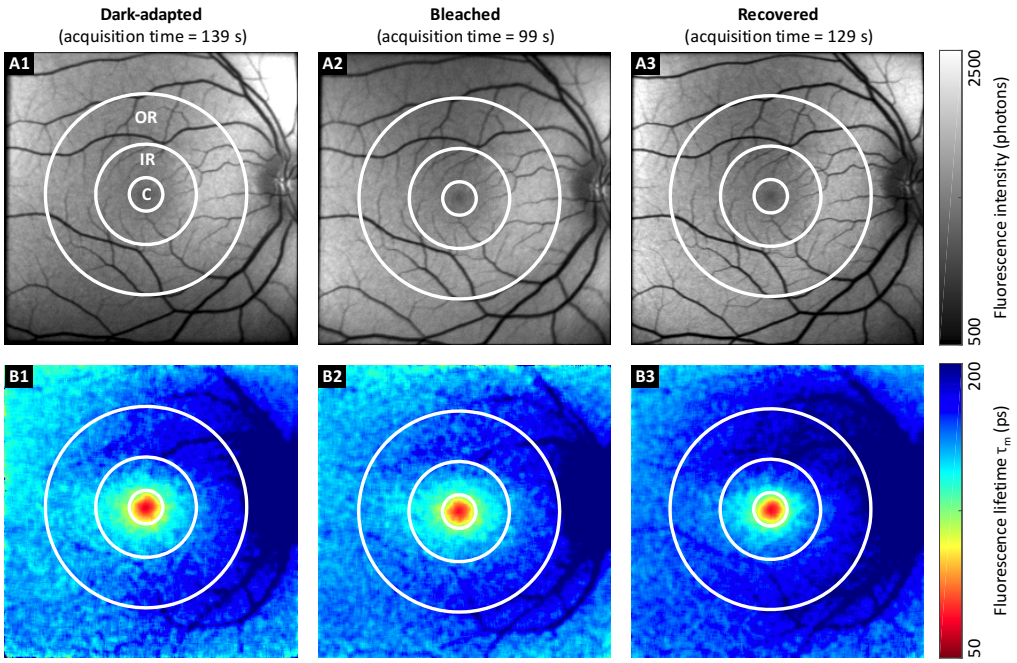

Fig. 3. FAF intensity and lifetime images from SSC of a healthy volunteer. FAF intensity (A), and corresponding mean FAF lifetime images (B) for dark-adapted (1), bleached (2), and recovered (3) states in one healthy volunteer. Although the fluorescence intensity and lifetime images were very similar, the acquisition times differed significantly. The central area (C), inner ring (IR), and outer ring (OR) from the ETDRS grid were used for the data analysis (diameter 1, 3, and 6 mm, respectively). For better comparison, the color scaling is identical for the three fluorescence intensities, and the fluorescence lifetime plots.

For each region (central, IR, OR) from each measurement, the mean values of fluorescence amplitudes and lifetimes were used for further statistical evaluation. The Shapiro–Wilk test [36] was applied to determine if the values of the fluorescence amplitudes and lifetimes obtained from all participants followed a normal distribution. In the case of normally distributed measurements, a repeated measure analysis of variance (ANOVA) for dependent samples was applied to identify significant differences between dark-adapted, bleached, and recovered states. Otherwise, the Friedman test was utilized. The post hoc tests applied Bonferroni corrections.

Data analysis was performed using FLIMX [37], which is documented and freely available for download online under the open source BSD–license (http://www.flimx.de). SPSS 24 (SPSS, Inc., Chicago, IL, USA) was employed for statistical analyses, including ANOVA, Friedman, and post hoc tests.

3. Results

Except for the usual random variation between measurements, we could not find any systematic changes in the fluorescence intensity images in terms of pattern or contrast among the different states.

Figure 3 illustrates FAF intensity and mean lifetime images following dark adaptation, directly after bleaching, and at 10 min after bleaching for one typical study participant. Although acquisition times for the FLIO measurements at bleached states were much shorter (78 s) than the acquisition times at dark-adapted states (136 s) or recovered states (138 s), the number of detected photons and mean fluorescence lifetimes were very similar in all three measurements.

Biomedical Optics EXPRESS

Figure 4 depicts the FAF mean lifetime τ_m and its fluorescence lifetime components (τ_1 - τ_3) of the different bleaching states at different fundus locations in both spectral channels.

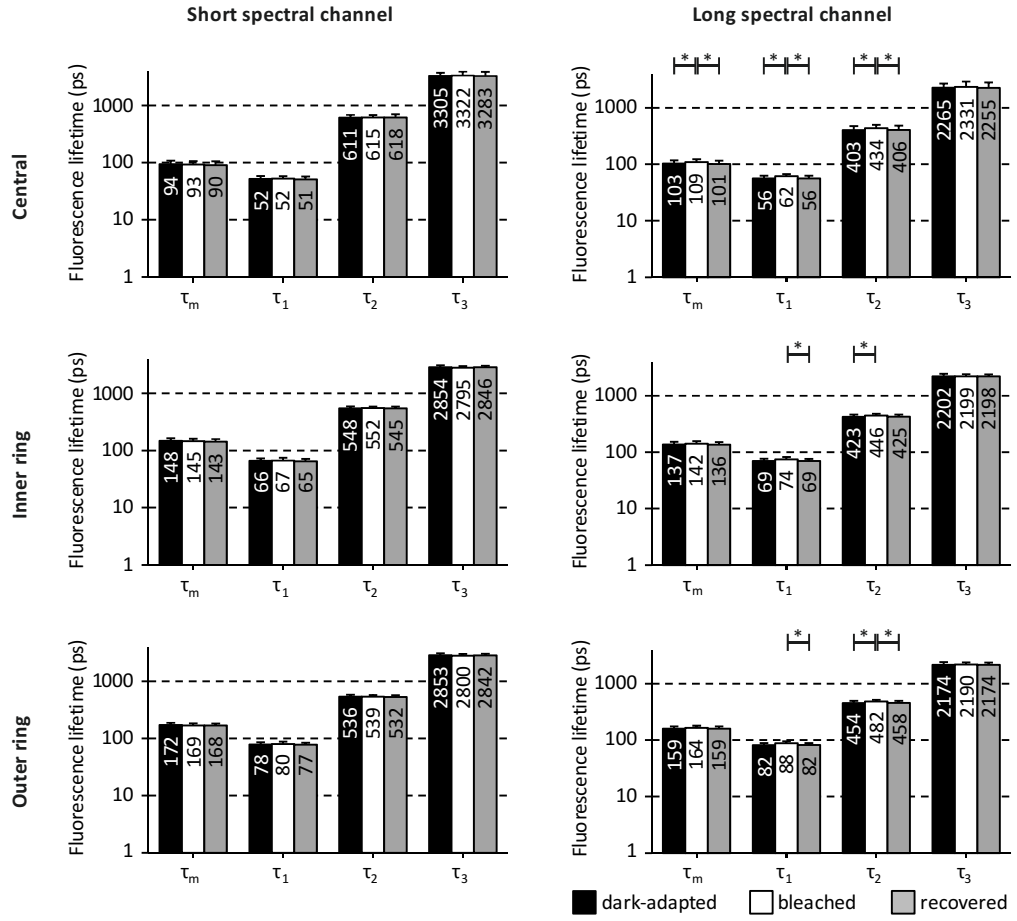

Fig. 4. Fluorescence lifetimes of the different bleaching states at different fundus locations. The fluorescence lifetimes are presented as mean ± standard deviation for both spectral channels in the central area, the inner ring, and the outer ring of the ETDRS grid. Significant differences are marked by * ($p < 0.05$). The differences between dark-adapted and bleached states of fluorescence lifetime τ_1 in the long spectral channel occurred at trend level for the outer ring ($p = 0.092$). The plots are on a logarithmic scale, and values are rounded to the nearest decimal.

The SSC did not show any significant alterations in the fluorescence lifetimes related to bleaching. There also were no significant differences in the fluorescence lifetime between the dark-adapted state and the recovered state in the SSC. However, some significant differences were found in the LSC. Fluorescence lifetimes τ_1 and τ_2 were slightly but significantly longer in the bleached state measurements compared to either dark-adapted state, and/or recovered state measurements. This applied to all three regions in the LSC. In the central area of the LSC, significant differences were also found for τ_m (dark-adapted state compared to bleached state: $p = 0.026$; bleached state compared to recovered state: $p = 0.01$). However, all of these fluorescence lifetime changes were less than 10%, which is only a minor alteration.

Figure 5 shows Bonferroni-corrected confidence intervals (confidence level 95%) of the pairwise fluorescence lifetime differences between the different bleaching states at different fundus locations, as recommended by the CONSORT Group [38]. The confidence intervals indicate the precision of the estimated bleaching effect on the fluorescence lifetimes.

Biomedical Optics EXPRESS

Significant differences, indicated by the confidence interval not including zero, are found in different fluorescence lifetime measures, including the mean fluorescence lifetime τ_m between the dark-adapted state and bleached state in the LSC.

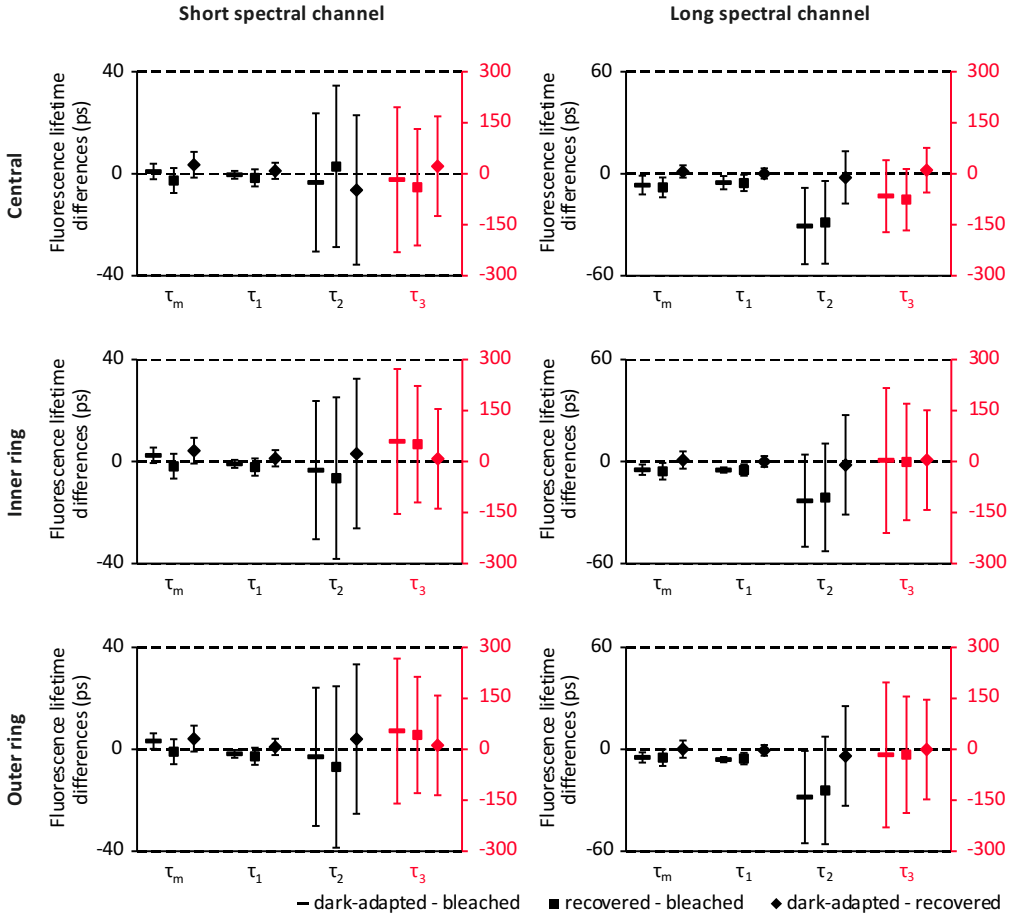

Fig. 5. Bonferroni-corrected confidence intervals (confidence level 95%) of the pairwise fluorescence lifetime differences between the different bleaching states at different fundus locations. The scale for confidence intervals of the fluorescence lifetime τ_3 is adjusted for better visibility (red). The confidence interval not including zero indicates a significant difference.

The average acquisition times for dark-adapted (128 s) and recovered (132 s) states were very similar, while the bleached measurements required significantly less time (104 s, $p < 0.05$) to obtain a similar amount of photons. On average, measurements in the bleached state were approximately 20% faster than measurements in dark-adapted and recovery states. To correct for a possible variation in detected fluorescence intensity of the different measurements, the total number of detected photons per pixel was divided by the acquisition time, averaged over the region of interest, and then averaged over the volunteers to obtain an approximate of acquisition speed per measurement (Fig. 6).

Biomedical Optics EXPRESS

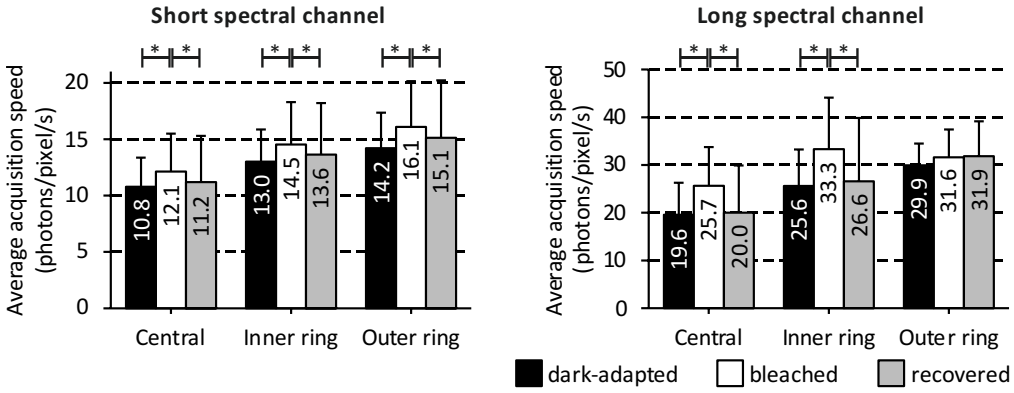

Fig. 6. Average acquisition speeds for the different bleaching states at the different fundus locations. The acquisition speeds are plotted as mean ± standard deviation for both spectral channels in the central area, the inner ring, and the outer ring of the ETDRS grid. Significant differences are marked by * ($p < 0.05$).

4. Discussion

The novel technique of fluorescence lifetime imaging is transitioning from a research device to a clinically used application, and basic research studies to improve the understanding of this technique are indispensable. As it is impossible to control for light exposure in a clinical setting, the understanding if or how light may potentially influence the FLIO method is necessary. This work particularly describes the effect of light bleaching at high light intensities compared to extensive dark adaptation on FLIO.

Overall, bleaching of the human retina significantly shortens the acquisition time, but has no effect on the fluorescence lifetimes within the SSC. A very small but significant effect on the fluorescence lifetimes within the LSC was found. This prolongation, depicted in Fig. 4, is minor compared to the overall lifetime and likely falls within lifetime changes that are accepted in other studies as normal variation. In previous studies, the inter-individual variability of fluorescence lifetime values quantified with the coefficient of variation were found to be between 6% and 17% [11]. All of the fluorescence lifetime changes reported with regards to bleaching were less than 10%. Therefore, it is reasonable to argue that these alterations will not or only marginally affect clinical applications.

Nevertheless, as we found these significant changes, it is appropriate to discuss why FAF lifetimes may be slightly altered with bleaching. One may argue that the macular pigment, retinal carotenoids accumulating in the fovea, may have an impact. However, these pigments are distributed in an area of 1 mm in diameter at the fovea due to the presence of macular pigment binding proteins, and their fluorescence emission is mostly found in the SSC [24,25,39]. The SSC shows no significant changes in the fluorescence lifetime with bleaching. Additionally, photobleaching of the macular pigment itself is not known [40]. Since significant differences in fluorescence lifetimes were predominantly found in the central macula within the LSC, different bleaching characteristics for rods and cones might be assumed. The white bleaching light, however, should bleach all photopigments in a similar way. Furthermore, the minor prolongation of fluorescence lifetimes in the LSC might be explained by a higher contribution of retinal pigment epithelium fluorescence to the overall fluorescence signal of the retina in this spectral channel. The regeneration of photopigments causes an accumulation of bisretinoid pigments in the RPE cells known as lipofuscin, which are fluorescent byproducts of the visual cycle [4,5,41,42]. Lipofuscin emits a bi-exponential fluorescence decay signal with a mean fluorescence lifetime of 1352 ps [18], which is longer than the fluorescence lifetime τ_2 and shorter than the fluorescence lifetime τ_3 in our measurements. A2E, one of the lipofuscin bisretinoids, possesses a short fluorescence lifetime component of 170 ps [18]. In addition to lipofuscin, the RPE emits a fluorescence signal from

Biomedical Optics EXPRESS

melanosomes with a short fluorescence lifetime found by Miura et al. [43] and Peters et al. [44]. They took samples from young pigs, which have almost no lipofuscin in their RPE cells and no macular pigment [45]. Therefore, a fluorescence signal from lipofuscin with a longer fluorescence lifetime is not present in their data. Thus, a higher contribution of the RPE fluorescence signal, originating from melanosomes and lipofuscin, caused by bleaching of the photopigments could prolong the fluorescence lifetimes τ_1 and τ_2. Therefore, the bisretinoid accumulation might be an interesting theory to follow upon. However, our study population shows a mean age of 24 years, where bisretinoid accumulations are unlikely to play a significant role.

The similarity of fluorescence lifetimes as well as acquisition times between dark-adapted and recovery measurements confirm our theory that the photoreceptor pigments are largely regenerated during the 10 minutes of recovery time. This finding is in accordance to the literature [22,23].

In addition to the bleaching of the photopigments, any other protein-based fluorophore in the retina may be also photobleached. Dynamic photobleaching processes chemically destroy fluorescent molecules upon exposure to excitation light [46]. As a result, these molecules lose their ability to fluoresce. Fluorescence measurement techniques used in microscopy, such as fluorescence photobleaching recovery [47], are based on this effect. In vitro studies revealed that irradiation of A2E, a characterized lipofuscin bisretinoid [48], was associated with photo-oxidation, photoisomerization, and photodegradation [49–51], resulting in reduced A2E fluorescence which did not fully recover within 24 hours. A2-PE, another bisretinoid, also seems to be susceptible to photochemical reactions [52]. In addition, it cannot be excluded that bleaching processes of the light sensitive fluorophore riboflavin might influence our results. The fluorescence spectrum of riboflavin is located primarily in LSC.

The results of our study suggest that dynamic light exposure and associated photobleaching of retinal fluorophores does not interfere with FLIO measurements. In addition, photobleaching of fluorophores would likely result in a reduced fluorescence intensity signal, whereas we found an increased signal for the bleached state. Although significantly longer fluorescence lifetimes were found in the bleached state compared to the dark-adapted or recovered state, mostly for the intermediate fluorescence lifetime component τ_2, the relevance of these differences is highly questionable. These changes presented in the order of only a few picoseconds, which is negligible compared to the differences found between controls and patients in recent clinical studies. A comparison is reported in Table 1.

Biomedical Optics EXPRESS

Table 1. Fluorescence lifetime changes in patients with different diseases compared to the present work[a]

Disease	Parameter	Change in fluorescence lifetime	Region for comparison (this work)	Effect of bleaching (this work)
AMD with geographic atrophy [53]	τ_m	+418 ps in atrophic areas vs. surrounding tissue	OR	+5 ps (LSC)
AMD with reticular pseudodrusen and / or soft drusen [54]	τ_m	+175 ps in patients vs. controls	OR	+5 ps (LSC)
Nonexudative AMD [15]	τ_m	+79 ps in patients vs. controls	OR	+5 ps (LSC)
Diabetes without diabetic retinopathy [16]	τ_3	+280 ps in patients vs. controls	OR	+16 ps (LSC)
Non-proliferative diabetic retinopathy [55]	τ_m	+25 ps in patients vs. controls	C	+8 ps (LSC)
Branch retinal artery occlusion [56]	τ_1	+85 ps in ischemic areas vs. unaffected areas	OR	+6 ps (LSC)
Central retinal artery occlusion [57]	τ_m	+89 ps in patients vs. controls	IR	+6 ps (LSC)
Macular holes without operculum [58]	τ_m	+63 ps in patients vs. controls	C	+8 ps (LSC)
Stargardt's disease [59]	τ_m	+149 ps in hyperfluorescent flecks vs. surrounding tissue +77 ps in atrophic areas vs. surrounding tissue	OR	+5 ps (LSC)
Macular Telangiectasia Type 2 [17]	τ_m	+90 ps in patients (early stage) vs. controls	IR	+3 ps (SSC)
Retinitis Pigmentosa [60]	τ_m	+89 ps in patients vs. controls	IR	+6 ps (LSC)
Retinitis Pigmentosa [61]	τ_m	+118 ps in patients vs. controls	OR	+5 ps (LSC)

Even small differences in fluorescence lifetimes of patients compared to healthy subjects, such as in patients with non-proliferative diabetic retinopathy, still are larger than bleaching-related differences.

Furthermore, it is important to point out that photopigment bleaching in this work was very intensive, using high amounts of light to make sure that bleaching is effective. The bleaching-related differences reported in this work are expected to be much larger than any differences caused by different ambient light conditions in a clinical environment. One may argue that previous clinical imaging may play a role in terms of photopigment bleaching. However, we were able to show that bleaching effects are reversible within a few minutes, which often accounts for the time patients take to transition between different imaging devices. Thus, the bleaching state of the photopigments is considered to have no major influence on fluorescence lifetimes measured in the clinical setting. Future FLIO studies that rely on very small differences in the fluorescence lifetime, e.g. studies investigating early disease detection, may have to consider the photopigment bleaching state of the patients in the study design.

There are some limitations in our study. It was impossible to document the exact time delay between bleaching and the FLIO measurement immediately after bleaching. This time, although not documented, was less than 10 seconds. The photoreceptor pigments may also be bleached by the excitation laser during the first 20–30 s of each (dark-adapted) FLIO

Biomedical Optics EXPRESS

measurement, which is short in comparison to FLIO's average acquisition time of circa 130 s. Thus, the effect of bleaching on FLIO is considerably small. The effect may increase with shorter acquisition times, which should be considered in the ongoing discussion of shortening the FLIO acquisition time. The acquisition times in general are not directly comparable between FLIO measurements, as each measurement is manually stopped by the operator once the threshold of 1000 photons per pixel is reached. The course of the photon count rates over time during FLIO measurements could not be recorded owing to technical limitations. This might be helpful in future measurements to evaluate if a possible bleaching caused by the FLIO device increases the fluorescence signal from the RPE. The validity of such assumption is based on the expectation that the photon count rates would increase exponentially during the first seconds of the dark-adapted measurements, in a similar manner to the findings reported by Theelen et al. [62]. The results of our study are reported in a very young group of volunteers. Findings might be different for older volunteers or for patients, especially with pathologic changes in the photoreceptor system and the lipofuscin content.

We also want to note two difficulties regarding to the estimation of photopigment bleaching level. First, the use of a single (photopic) light measurement cannot correctly calculate the bleaching for both, the red-sensitive and green-sensitive (M and L) cones. However, the approach should be reasonably accurate in the case of white light, as was used in this study for bleaching. Second, with pupil dilation, calculations employing raw troland values are bound to overestimate the absorption of light by the cones because of the Stiles–Crawford effect [63]. Thus, much of the light that enters the pupil near its rim will be ineffective in exciting (or bleaching) the cones, yet will be included in the troland calculation.

In future work, the bleaching effect of FLIO's excitation laser will be investigated by bleaching using the excitation wavelength, in comparison to bleaching with white light.

5. Conclusion

Differences in fluorescence lifetimes caused by photopigment bleaching are comparable to general inter-individual variations. It therefore is safe to conclude that bleaching has a negligible influence on FLIO measurements. Bleaching of retinal photoreceptors will not interfere with FLIO patterns that were reported for various eye diseases. Thus, patients should not be bleached prior to FLIO measurements to keep their stress levels as low as possible. However, it is reasonable to suggest that FLIO users should attempt to follow an acquisition protocol in research studies to obtain the most reliable results with regards to photopigment bleaching state. Within 10 minutes of any light exposure patients may experience in the clinical routine, fluorescence lifetime characteristics will return to baseline values. Overall, photopigment bleaching likely has no influence on the outcome and overall FLIO measurement in the clinical setting.

Funding

German Federal Ministry of Education and Research (BMBF 03IPT605X); German Research Foundation (DFG Ha 2899/19-1); Carl Zeiss Foundation, German Research Foundation (DFG); Open Access Publication Fund of the Technische Universität Ilmenau.

Acknowledgements

The authors would like to thank all participants of this study. The authors also thank Heidelberg Engineering for providing the FLIO device and technical assistance, as well as Lowy Medical Research Institute (LMRI) for their support.

Disclosures

The authors declare that there are no conflicts of interest related to this article.

Biomedical Optics EXPRESS

References

1. S. Schmitz-Valckenberg, F. G. Holz, A. C. Bird, and R. F. Spaide, "Fundus autofluorescence imaging: review and perspectives," Retina **28**(3), 385–409 (2008).
2. F. C. Delori, C. K. Dorey, G. Staurenghi, O. Arend, D. G. Goger, and J. J. Weiter, "In vivo fluorescence of the ocular fundus exhibits retinal pigment epithelium lipofuscin characteristics," Invest. Ophthalmol. Vis. Sci. **36**(3), 718–729 (1995).
3. J. R. Sparrow, E. Gregory-Roberts, K. Yamamoto, A. Blonska, S. K. Ghosh, K. Ueda, and J. Zhou, "The bisretinoids of retinal pigment epithelium," Prog. Retin. Eye Res. **31**(2), 121–135 (2012).
4. J. R. Sparrow, Y. Wu, T. Nagasaki, K. D. Yoon, K. Yamamoto, and J. Zhou, "Fundus autofluorescence and the bisretinoids of retina," Photochem. Photobiol. Sci. **9**(11), 1480–1489 (2010).
5. J. R. Sparrow, Y. Wu, C. Y. Kim, and J. Zhou, "Phospholipid meets all-trans-retinal: the making of RPE bisretinoids," J. Lipid Res. **51**(2), 247–261 (2010).
6. T. Ben Ami, Y. Tong, A. Bhuiyan, C. Huisingh, Z. Ablonczy, T. Ach, C. A. Curcio, and R. T. Smith, "Spatial and Spectral Characterization of Human Retinal Pigment Epithelium Fluorophore Families by Ex Vivo Hyperspectral Autofluorescence Imaging," Transl. Vis. Sci. Technol. **5**(3), 5 (2016).
7. D. Schweitzer, E. R. Gaillard, J. Dillon, R. F. Mullins, S. Russell, B. Hoffmann, S. Peters, M. Hammer, and C. Biskup, "Time-resolved autofluorescence imaging of human donor retina tissue from donors with significant extramacular drusen," Invest. Ophthalmol. Vis. Sci. **53**(7), 3376–3386 (2012).
8. C. Dysli, S. Wolf, M. Y. Berezin, L. Sauer, M. Hammer, and M. S. Zinkernagel, "Fluorescence lifetime imaging ophthalmoscopy," Prog. Retin. Eye Res. **60**, 120–143 (2017).
9. L. Sauer, K. M. Andersen, C. Dysli, M. S. Zinkernagel, P. S. Bernstein, and M. Hammer, "Review of clinical approaches in fluorescence lifetime imaging ophthalmoscopy," J. Biomed. Opt. **23**(9), 1–20 (2018).
10. M. Klemm, A. Dietzel, J. Haueisen, E. Nagel, M. Hammer, and D. Schweitzer, "Repeatability of autofluorescence lifetime imaging at the human fundus in healthy volunteers," Curr. Eye Res. **38**(7), 793–801 (2013).
11. C. Dysli, G. Quellec, M. Abegg, M. N. Menke, U. Wolf-Schnurrbusch, J. Kowal, J. Blatz, O. La Schiazza, A. B. Leichtle, S. Wolf, and M. S. Zinkernagel, "Quantitative analysis of fluorescence lifetime measurements of the macula using the fluorescence lifetime imaging ophthalmoscope in healthy subjects," Invest. Ophthalmol. Vis. Sci. **55**(4), 2106–2113 (2014).
12. D. Schweitzer, M. Hammer, F. Schweitzer, R. Anders, T. Doebbecke, S. Schenke, E. R. Gaillard, and E. R. Gaillard, "In vivo measurement of time-resolved autofluorescence at the human fundus," J. Biomed. Opt. **9**(6), 1214–1222 (2004).
13. J. R. Lakowicz, *Principles of Fluorescence Spectroscopy,* 3rd ed. (Springer, New York, 2006), p. 954.
14. W. Becker, "Fluorescence lifetime imaging--techniques and applications," J. Microsc. **247**(2), 119–136 (2012).
15. L. Sauer, R. H. Gensure, K. M. Andersen, L. Kreilkamp, G. S. Hageman, M. Hammer, and P. S. Bernstein, "Patterns of Fundus Autofluorescence Lifetimes In Eyes of Individuals With Nonexudative Age-Related Macular Degeneration," Invest. Ophthalmol. Vis. Sci. **59**(4), AMD65–AMD77 (2018).
16. D. Schweitzer, L. Deutsch, M. Klemm, S. Jentsch, M. Hammer, S. Peters, J. Haueisen, U. A. Müller, and J. Dawczynski, "Fluorescence lifetime imaging ophthalmoscopy in type 2 diabetic patients who have no signs of diabetic retinopathy," J. Biomed. Opt. **20**(6), 61106 (2015).
17. L. Sauer, R. H. Gensure, M. Hammer, and P. S. Bernstein, "Fluorescence Lifetime Imaging Ophthalmoscopy: A Novel Way to Assess Macular Telangiectasia Type 2," Ophthalmol. Retina **2**(6), 587–598 (2018).
18. D. Schweitzer, S. Schenke, M. Hammer, F. Schweitzer, S. Jentsch, E. Birckner, W. Becker, and A. Bergmann, "Towards metabolic mapping of the human retina," Microsc. Res. Tech. **70**(5), 410–419 (2007).
19. D. Schweitzer, "Autofluorescence diagnostics of ophthalmic diseases," in *Natural Biomarkers for Cellular Metabolism: Biology, Techniques, and Applications,* 1 ed., V. V. Ghukasyan and A. A. Heikal, eds. (CRC Press, 2018), pp. 317–344.
20. M. Y. Loguinova, V. E. Zagidullin, T. B. Feldman, Y. V. Rostovtseva, V. Z. Paschenko, A. B. Rubin, and A. A. Ostrovsky, "Spectral Characteristics of Fluorophores Formed via Interaction between All-trans-Retinal with Rhodopsin and Lipids in Photoreceptor Membrane of Retina Rod Outer Segments," Биол. мембраны **26**, 83–93 (2009).
21. F. Delori, J. P. Greenberg, R. L. Woods, J. Fischer, T. Duncker, J. Sparrow, and R. T. Smith, "Quantitative measurements of autofluorescence with the scanning laser ophthalmoscope," Invest. Ophthalmol. Vis. Sci. **52**(13), 9379–9390 (2011).
22. W. A. H. Rushton and G. H. Henry, "Bleaching and regeneration of cone pigments in man," Vision Res. **8**(6), 617–631 (1968).
23. O. A. R. Mahroo and T. D. Lamb, "Recovery of the human photopic electroretinogram after bleaching exposures: estimation of pigment regeneration kinetics," J. Physiol. **554**(Pt 2), 417–437 (2004).
24. L. Sauer, K. M. Andersen, B. Li, R. H. Gensure, M. Hammer, and P. S. Bernstein, "Fluorescence Lifetime Imaging Ophthalmoscopy (FLIO) of Macular Pigment," Invest. Ophthalmol. Vis. Sci. **59**(7), 3094–3103 (2018).
25. L. Sauer, D. Schweitzer, L. Ramm, R. Augsten, M. Hammer, and S. Peters, "Impact of Macular Pigment on Fundus Autofluorescence Lifetimes," Invest. Ophthalmol. Vis. Sci. **56**(8), 4668–4679 (2015).
26. D. Schweitzer, "Metabolic mapping," in *Medical Retina: Focus on Retinal Imaging (Essentials in Ophthalmology)*, F. G. Holz and R. F. Spaide, eds. (Springer, Heidelberg, 2010), pp. 107–123.

Biomedical Optics EXPRESS

27. A. N. S. Institute and L. I. o. America, *American National Standard for Safe Use of Lasers (ANSI Z136.1)* (Laser Institute of America, 2007).
28. W. Becker, *Advanced Time-Correlated Single Photon Counting Techniques*, Springer series in chemical physics, (Springer, Berlin, 2005), p. 401.
29. W. Becker, *The bh TCPSC Handbook,* 5th ed. (Becker & Hickl GmbH, 2012), p. 690.
30. M. Hollins and M. Alpern, "Dark adaptation and visual pigment regeneration in human cones," J. Gen. Physiol. **62**(4), 430–447 (1973).
31. A. A. V. Paupoo, O. A. R. Mahroo, C. Friedburg, and T. D. Lamb, "Human cone photoreceptor responses measured by the electoretinogram a-wave during and after exposure to intense illumination," J. Physiol. **529**(2), 469–482 (2000).
32. D. C. Coile and H. D. Baker, "Foveal dark adaptation, photopigment regeneration, and aging," Vis. Neurosci. **8**(1), 27–39 (1992).
33. J. A. Nelder and R. Mead, "A Simplex-Method for Function Minimization," Comput. J. **7**(4), 308–313 (1965).
34. J. Neyman and E. S. Pearson, "On the Use and Interpretation of Certain Test Criteria for Purposes of Statistical Inference," Biometrika **20A**, 263–294 (1928).
35. Early Treatment Diabetic Retinopathy Study Research Group, "Grading diabetic retinopathy from stereoscopic color fundus photographs--an extension of the modified Airlie House classification. ETDRS report number 10," Ophthalmology **98**(5 Suppl), 786–806 (1991).
36. S. S. Shapiro and M. B. Wilk, "An Analysis of Variance Test for Normality (Complete Samples)," Biometrika **52**(3-4), 591–611 (1965).
37. M. Klemm, D. Schweitzer, S. Peters, L. Sauer, M. Hammer, and J. Haueisen, "FLIMX: A Software Package to Determine and Analyze the Fluorescence Lifetime in Time-Resolved Fluorescence Data from the Human Eye," PLoS One **10**(7), e0131640 (2015).
38. D. Moher, S. Hopewell, K. F. Schulz, V. Montori, P. C. Gøtzsche, P. J. Devereaux, D. Elbourne, M. Egger, and D. G. Altman, "CONSORT 2010 explanation and elaboration: updated guidelines for reporting parallel group randomised trials," BMJ **340**(mar23 1), c869 (2010).
39. M. Sharifzadeh, P. S. Bernstein, and W. Gellermann, "Nonmydriatic fluorescence-based quantitative imaging of human macular pigment distributions," J. Opt. Soc. Am. A **23**(10), 2373–2387 (2006).
40. A. J. Wenzel, K. Fuld, and J. M. Stringham, "Light exposure and macular pigment optical density," Invest. Ophthalmol. Vis. Sci. **44**(1), 306–309 (2003).
41. H. J. Kim and J. R. Sparrow, "Novel bisretinoids of human retina are lyso alkyl ether glycerophosphoethanolamine-bearing A2PE species," J. Lipid Res. **59**(9), 1620–1629 (2018).
42. J. R. Sparrow, K. Nakanishi, and C. A. Parish, "The lipofuscin fluorophore A2E mediates blue light-induced damage to retinal pigmented epithelial cells," Invest. Ophthalmol. Vis. Sci. **41**(7), 1981–1989 (2000).
43. Y. Miura, G. Huettmann, R. Orzekowsky-Schroeder, P. Steven, M. Szaszák, N. Koop, and R. Brinkmann, "Two-photon microscopy and fluorescence lifetime imaging of retinal pigment epithelial cells under oxidative stress," Invest. Ophthalmol. Vis. Sci. **54**(5), 3366–3377 (2013).
44. S. Peters, M. Hammer, and D. Schweitzer, "Two-photon excited fluorescence microscopy application for ex vivo investigation of ocular fundus samples," Proceedings of the SPIE - The International Society for Optical Engineering **8086**, 808605 (2011).
45. M. Hammer, L. Sauer, M. Klemm, S. Peters, R. Schultz, and J. Haueisen, "Fundus autofluorescence beyond lipofuscin: lesson learned from *ex vivo* fluorescence lifetime imaging in porcine eyes," Biomed. Opt. Express **9**(7), 3078–3091 (2018).
46. L. Song, E. J. Hennink, I. T. Young, and H. J. Tanke, "Photobleaching kinetics of fluorescein in quantitative fluorescence microscopy," Biophys. J. **68**(6), 2588–2600 (1995).
47. R. Peters, A. Brünger, and K. Schulten, "Continuous fluorescence microphotolysis: A sensitive method for study of diffusion processes in single cells," Proc. Natl. Acad. Sci. U.S.A. **78**(2), 962–966 (1981).
48. N. Sakai, J. Decatur, K. Nakanishi, and G. E. Eldred, "Ocular age pigment "A2-E": An unprecedented pyridinium bisretinoid," J. Am. Chem. Soc. **118**(6), 1559–1560 (1996).
49. K. Yamamoto, J. Zhou, J. J. Hunter, D. R. Williams, and J. R. Sparrow, "Toward an understanding of bisretinoid autofluorescence bleaching and recovery," Invest. Ophthalmol. Vis. Sci. **53**(7), 3536–3544 (2012).
50. Z. Liu, K. Ueda, H. J. Kim, and J. R. Sparrow, "Photobleaching and Fluorescence Recovery of RPE Bisretinoids," PLoS One **10**(9), e0138081 (2015).
51. M. Hammer, S. Richter, K. H. Guehrs, and D. Schweitzer, "Retinal pigment epithelium cell damage by A2-E and its photo-derivatives," Mol. Vis. **12**, 1348–1354 (2006).
52. S. R. Kim, K. Nakanishi, Y. Itagaki, and J. R. Sparrow, "Photooxidation of A2-PE, a photoreceptor outer segment fluorophore, and protection by lutein and zeaxanthin," Exp. Eye Res. **82**(5), 828–839 (2006).
53. C. Dysli, S. Wolf, and M. S. Zinkernagel, "Autofluorescence Lifetimes in Geographic Atrophy in Patients With Age-Related Macular Degeneration," Invest. Ophthalmol. Vis. Sci. **57**(6), 2479–2487 (2016).
54. C. Dysli, R. Fink, S. Wolf, and M. S. Zinkernagel, "Fluorescence Lifetimes of Drusen in Age-Related Macular Degeneration," Invest. Ophthalmol. Vis. Sci. **58**(11), 4856–4862 (2017).
55. J. Schmidt, S. Peters, L. Sauer, D. Schweitzer, M. Klemm, R. Augsten, N. Müller, and M. Hammer, "Fundus autofluorescence lifetimes are increased in non-proliferative diabetic retinopathy," Acta Ophthalmol. **95**(1), 33–40 (2017).

Biomedical Optics EXPRESS

56. D. Schweitzer, S. Quick, M. Klemm, M. Hammer, S. Jentsch, and J. Dawczynski, "[Time-resolved autofluorescence in retinal vascular occlusions]," Ophthalmologe **107**(12), 1145–1152 (2010).
57. C. Dysli, S. Wolf, and M. S. Zinkernagel, "Fluorescence lifetime imaging in retinal artery occlusion," Invest. Ophthalmol. Vis. Sci. **56**(5), 3329–3336 (2015).
58. L. Sauer, S. Peters, J. Schmidt, D. Schweitzer, M. Klemm, L. Ramm, R. Augsten, and M. Hammer, "Monitoring macular pigment changes in macular holes using fluorescence lifetime imaging ophthalmoscopy," Acta ophthalmologica, (2016).
59. C. Dysli, S. Wolf, K. Hatz, and M. S. Zinkernagel, "Fluorescence Lifetime Imaging in Stargardt Disease: Potential Marker for Disease Progression," Invest. Ophthalmol. Vis. Sci. **57**(3), 832–841 (2016).
60. K. M. Andersen, L. Sauer, R. H. Gensure, M. Hammer, and P. S. Bernstein, "Characterization of Retinitis Pigmentosa Using Fluorescence Lifetime Imaging Ophthalmoscopy (FLIO)," Transl. Vis. Sci. Technol. **7**(3), 20 (2018).
61. C. Dysli, K. Schürch, E. Pascal, S. Wolf, and M. S. Zinkernagel, "Fundus Autofluorescence Lifetime Patterns in Retinitis Pigmentosa," Invest. Ophthalmol. Vis. Sci. **59**(5), 1769–1778 (2018).
62. T. Theelen, T. T. J. M. Berendschot, C. J. F. Boon, C. B. Hoyng, and B. J. Klevering, "Analysis of visual pigment by fundus autofluorescence," Exp. Eye Res. **86**(2), 296–304 (2008).
63. W. S. Stiles and B. H. Crawford, "The Luminous Efficiency of Rays Entering the Eye Pupil at Different Points," Proc. R. Soc. Lond., B **112**(778), 428–450 (1933).